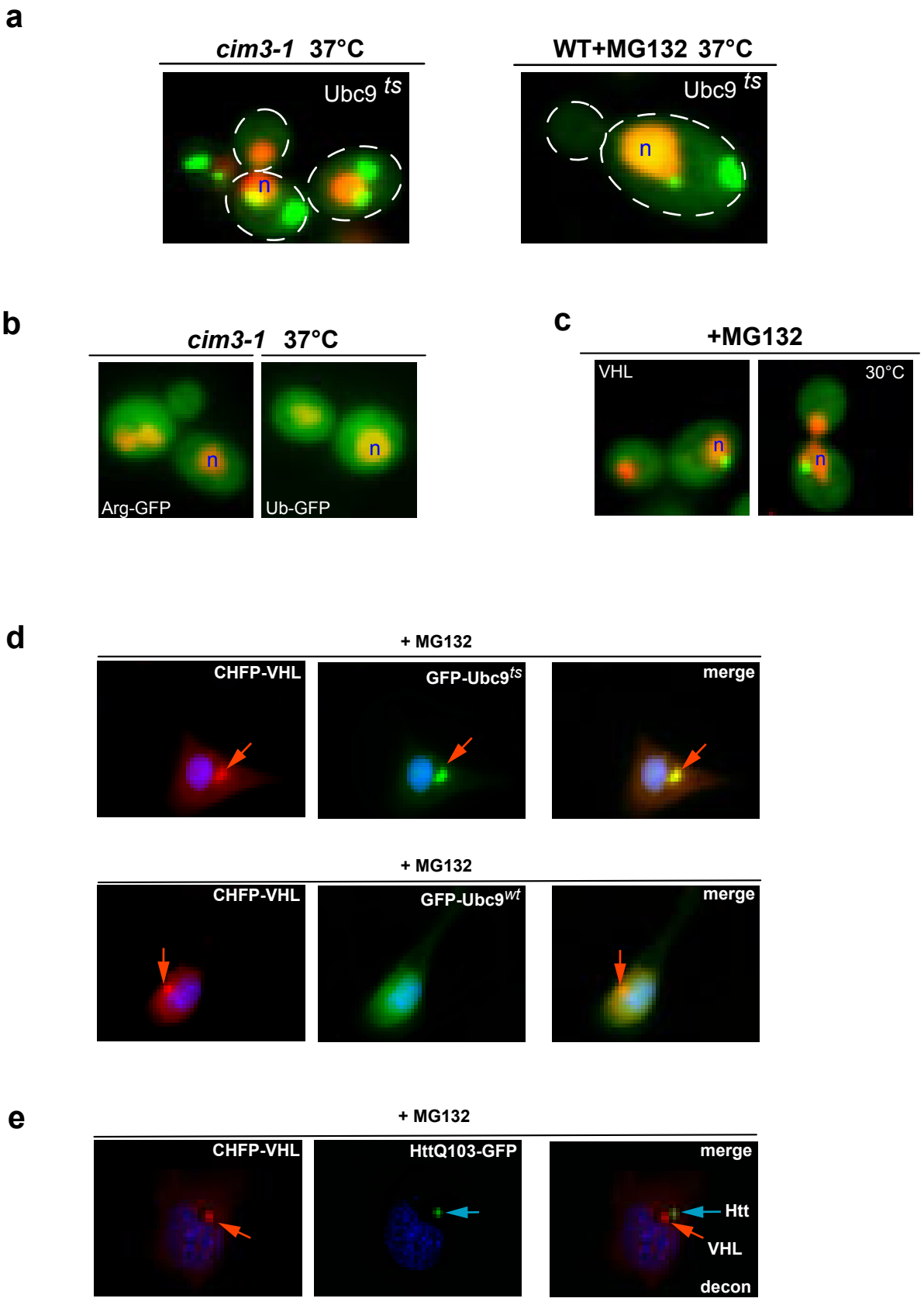
a
cim3-1 37°C
Ubc9 ts
n
WT+MG132 37°C
Ubc9 ts
n
b
cim3-1 37°C
n
Arg-GFP
n
Ub-GFP
c
+MG132
VHL
n
30°C
n
d
+ MG132
CHFP-VHL
GFP-Ubc9ts
merge
+ MG132
CHFP-VHL
GFP-Ubc9wt
merge
e
+ MG132
CHFP-VHL
HttQ103-GFP
merge
Htt
VHL
decon

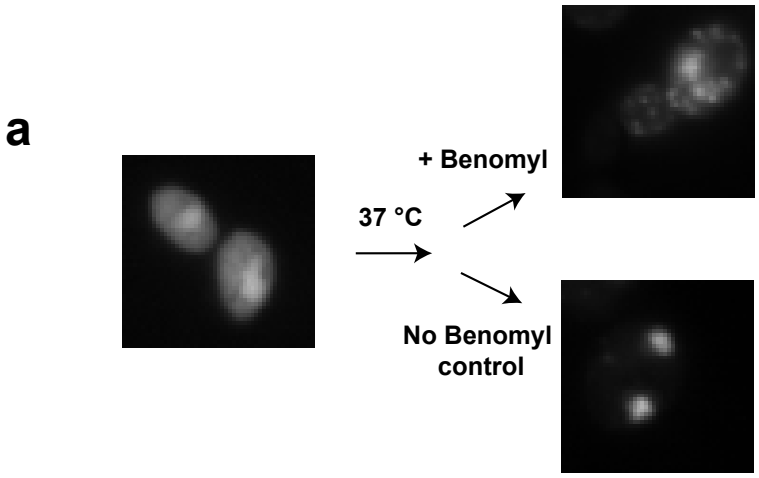
a
+ Benomyl
37 °C
No Benomyl
control

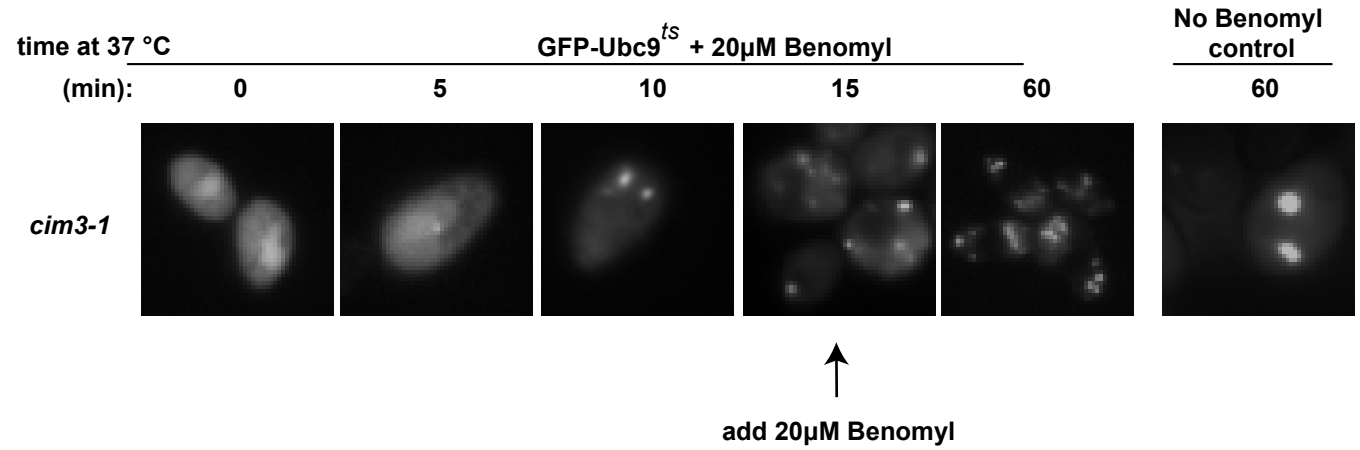
b
time at 37 °C
GFP-Ubc9ts + 20μM Benomyl
No Benomyl
control
(min):
0
5
10
15
60
60
cim3-1
add 20μM Benomyl

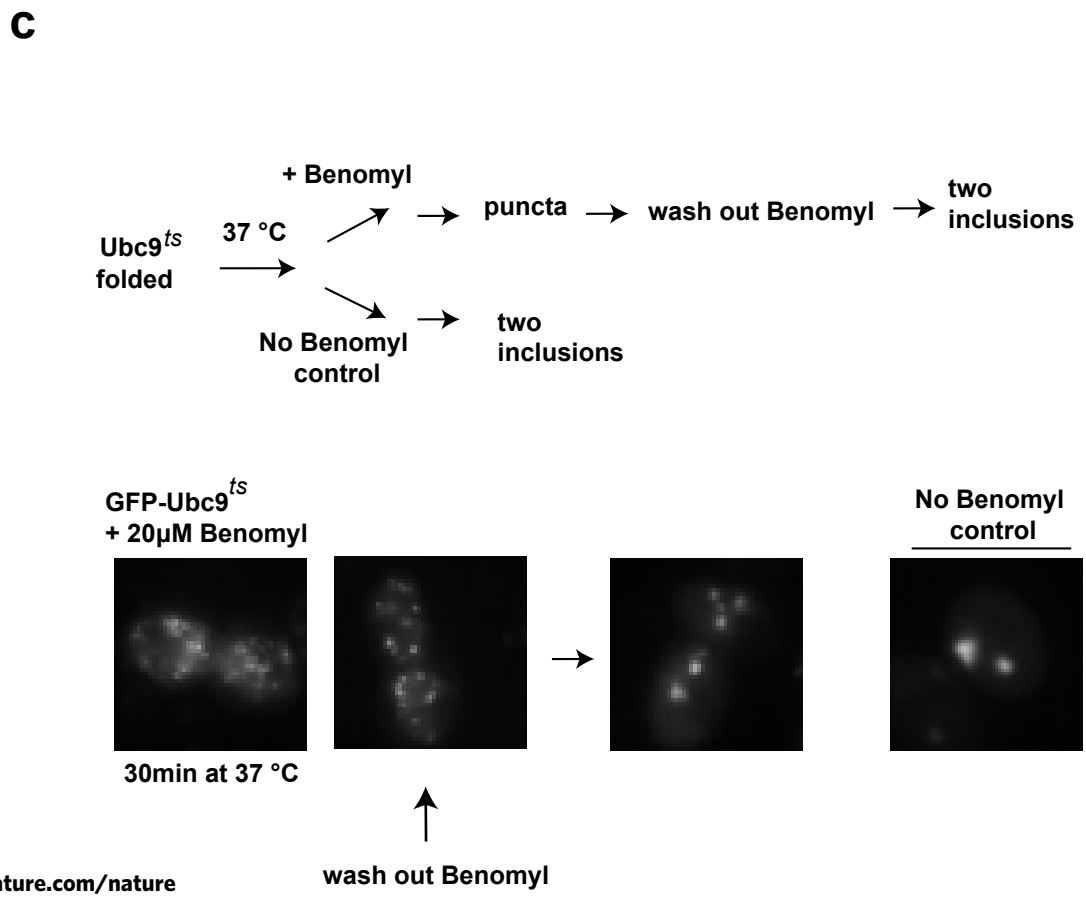
c
+ Benomyl
Ubc9ts
folded
37 °C
puncta
wash out Benomyl
two
inclusions
No Benomyl
control
two
inclusions
GFP-Ubc9ts
+ 20μM Benomyl
No Benomyl
control
30min at 37 °C
wash out Benomyl

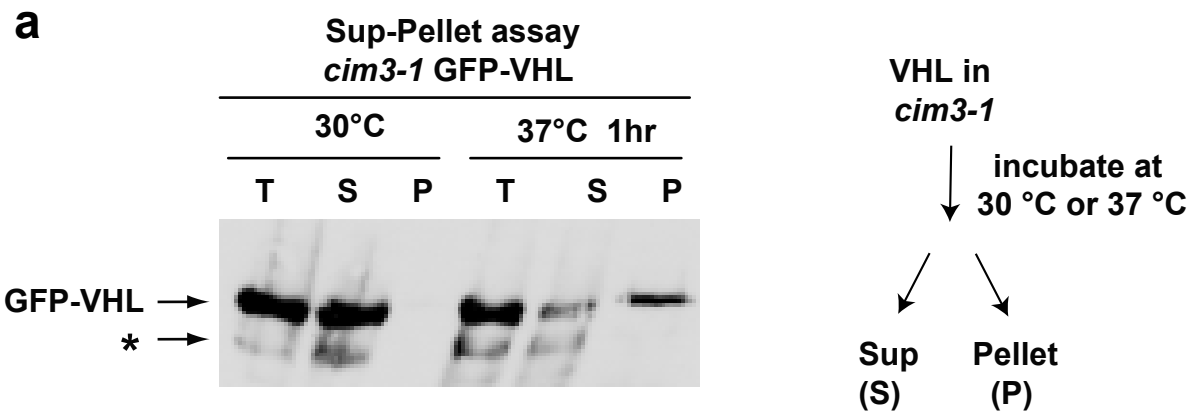
a
Sup-Pellet assay
cim3-1 GFP-VHL
30°C
37°C 1hr
T S P T S P
GFP-VHL
*
VHL in
cim3-1
incubate at
30 °C or 37 °C
Sup
(S)
Pellet
(P)

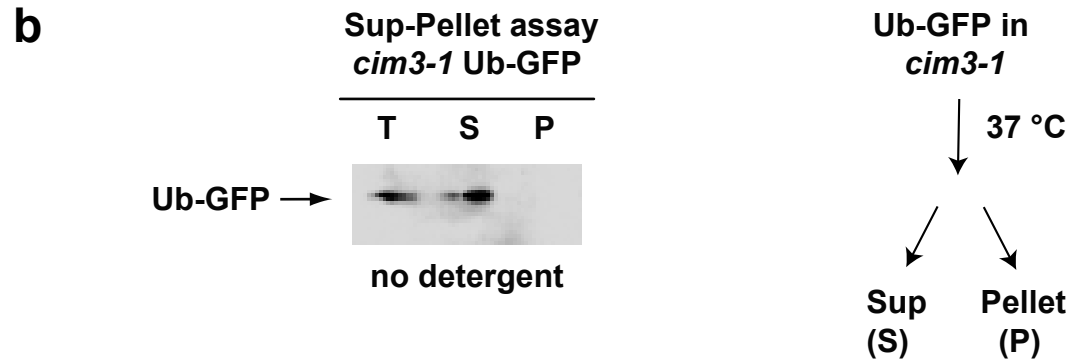
b
Sup-Pellet assay
cim3-1 Ub-GFP
T S P
Ub-GFP
no detergent
Ub-GFP in
cim3-1
37 °C
Sup
(S)
Pellet
(P)

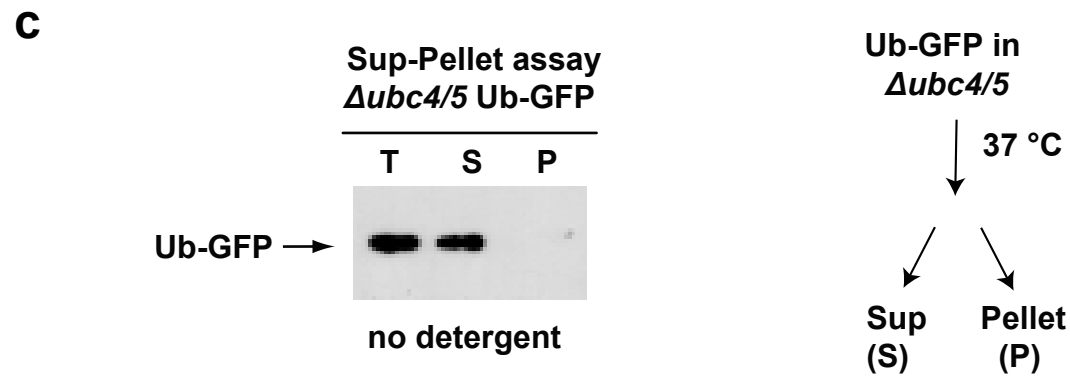
c
Sup-Pellet assay
Δubc4/5 Ub-GFP
T S P
Ub-GFP
no detergent
Ub-GFP in
Δubc4/5
37 °C
Sup
(S)
Pellet
(P)

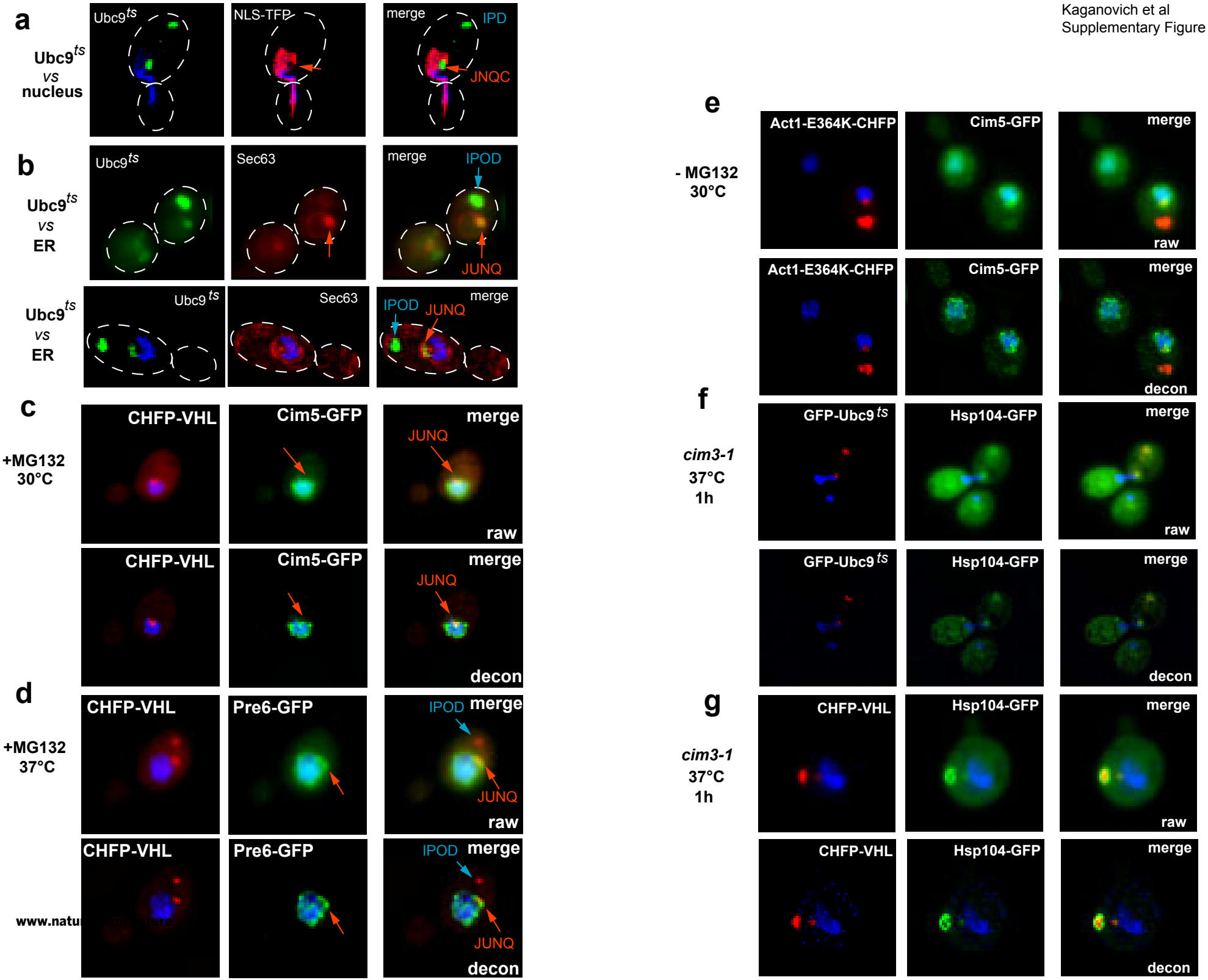
a
Ubc9ts vs nucleus
Ubc9ts
NLS-TFP
merge
IPD
JNQC
b
Ubc9ts vs ER
Ubc9ts
Sec63
merge
IPOD
JUNQ
Ubc9ts vs ER
Ubc9 ts
Sec63
IPOD
JUNQ
merge
c
+MG132 30°C
CHFP-VHL
Cim5-GFP
merge
JUNQ
raw
CHFP-VHL
Cim5-GFP
merge
JUNQ
decon
d
+MG132 37°C
CHFP-VHL
Pre6-GFP
IPOD
merge
JUNQ
raw
CHFP-VHL
Pre6-GFP
IPOD
merge
JUNQ
decon
www.natu
e
- MG132 30°C
Act1-E364K-CHFP
Cim5-GFP
merge
raw
Act1-E364K-CHFP
Cim5-GFP
merge
decon
f
cim3-1 37°C 1h
GFP-Ubc9 ts
Hsp104-GFP
merge
raw
GFP-Ubc9 ts
Hsp104-GFP
merge
decon
g
cim3-1 37°C 1h
CHFP-VHL
Hsp104-GFP
merge
raw
CHFP-VHL
Hsp104-GFP
merge
decon

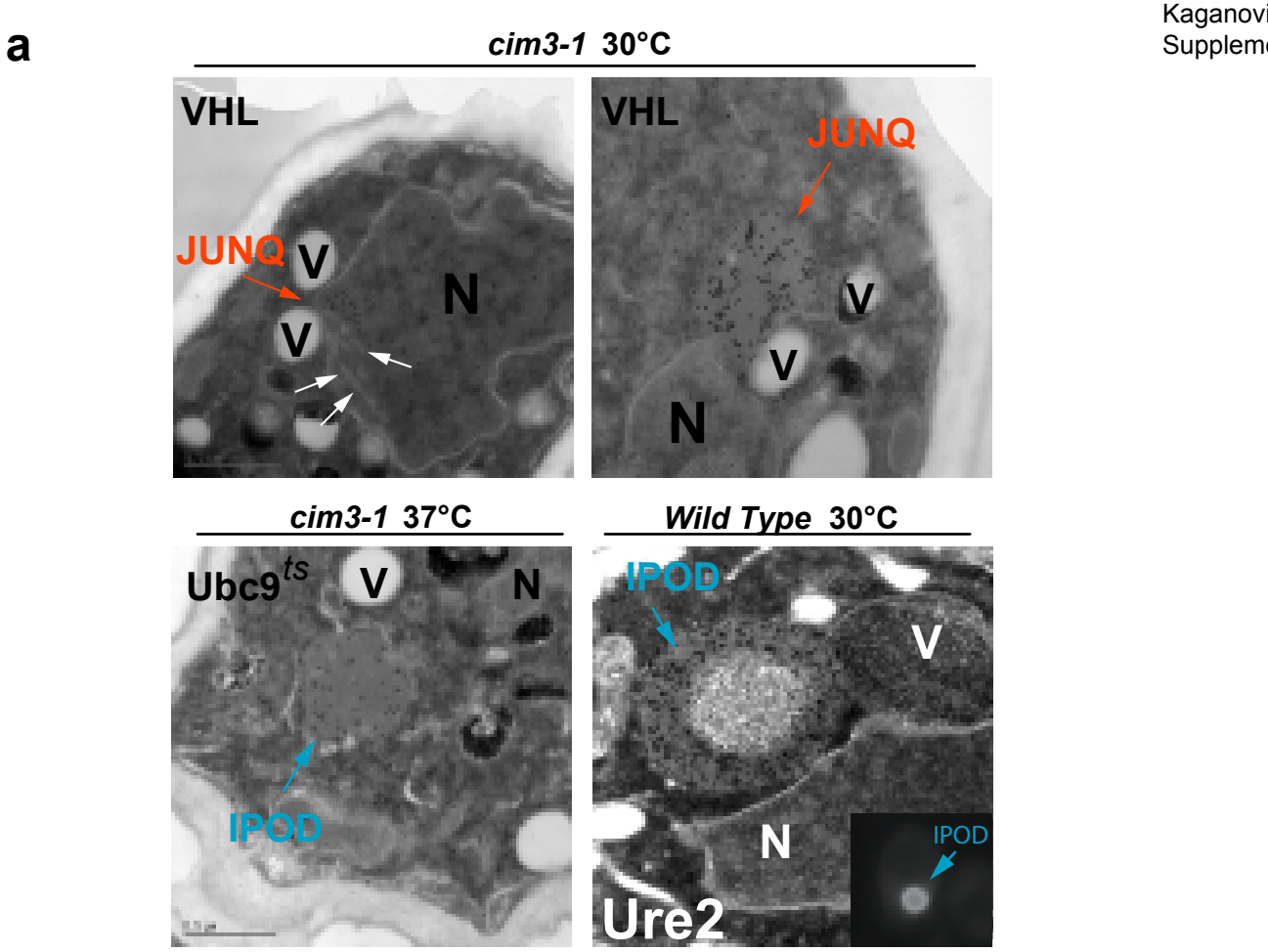
a
cim3-1 30°C
VHL
JUNQ
V
N
V
VHL
JUNQ
V
V
N
cim3-1 37°C
Ubc9ts
V
N
IPOD
Wild Type 30°C
IPOD
V
N
Ure2
IPOD

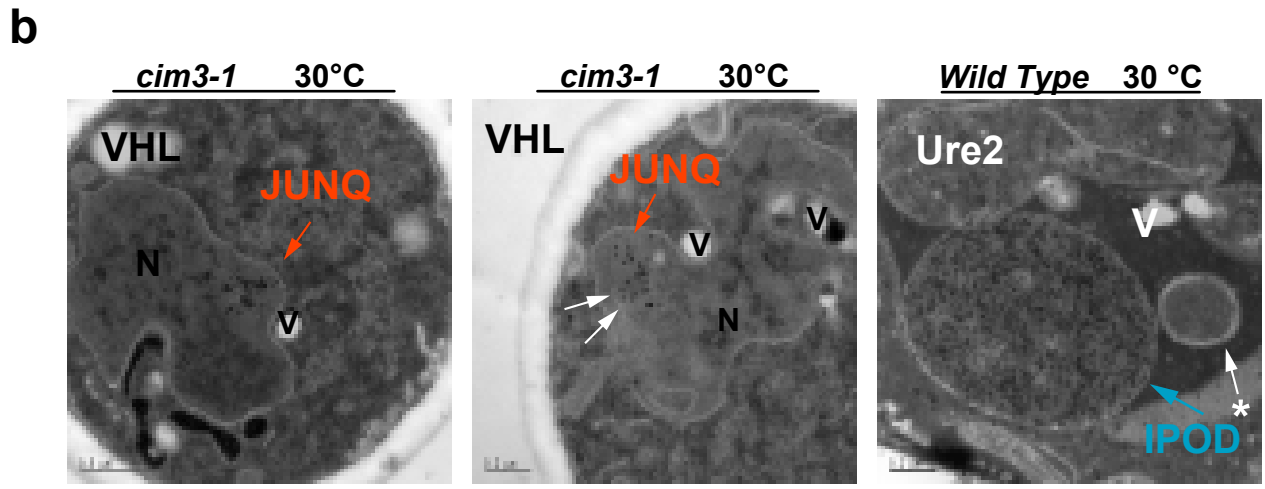
b
cim3-1 30°C
VHL
JUNQ
N
V
cim3-1 30°C
VHL
JUNQ
V
V
N
Wild Type 30 °C
Ure2
V
*
IPOD

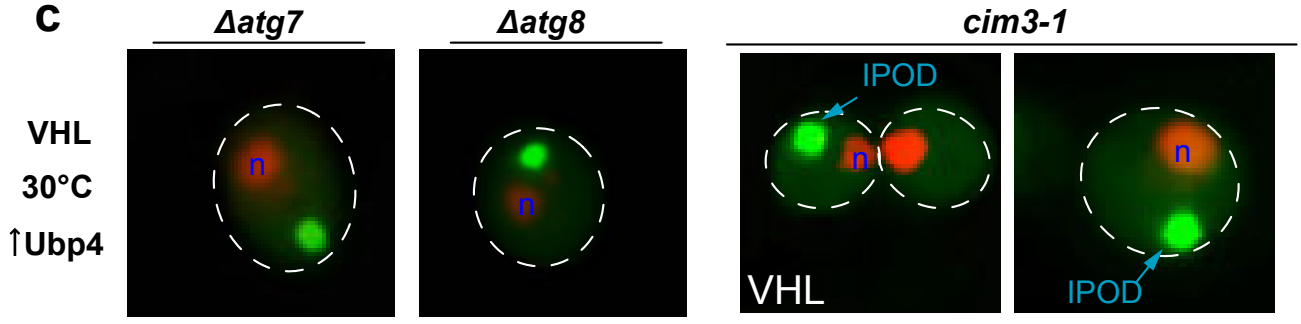
c
Δatg7
Δatg8
cim3-1
VHL
30°C
↑Ubp4
n
n
IPOD
n
VHL
n
IPOD

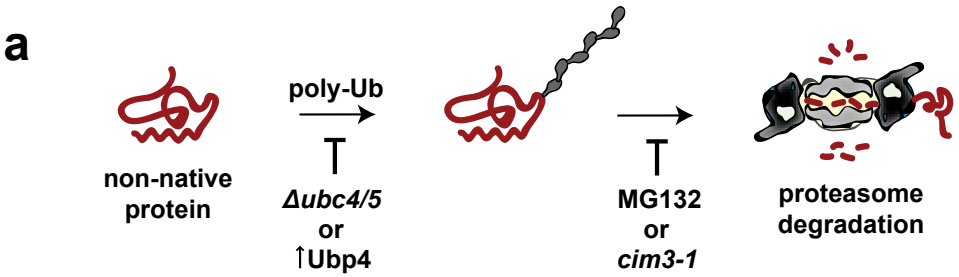
a
non-native protein
poly-Ub
Δubc4/5 or ↑Ubp4
MG132 or cim3-1
proteasome degradation

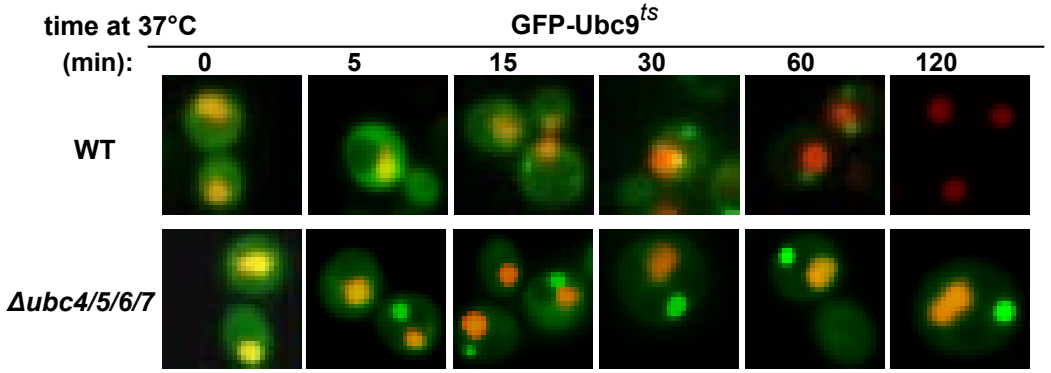
b
time at 37°C (min):
0
5
15
30
60
120
GFP-Ubc9ts
WT
Δubc4/5/6/7

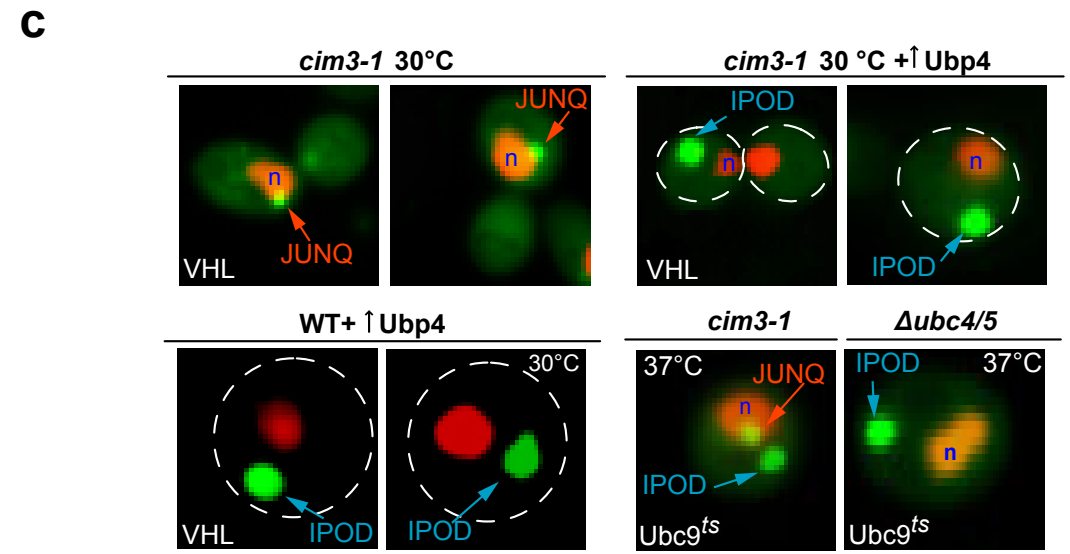
c
cim3-1 30°C
cim3-1 30 °C +↑Ubp4
JUNQ
IPOD
VHL
WT+ ↑Ubp4
30°C
cim3-1
Δubc4/5
37°C
Ubc9ts

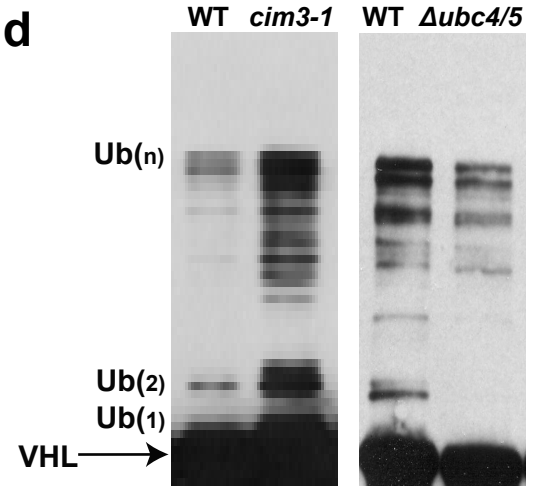
d
WT
cim3-1
WT
Δubc4/5
Ub(n)
Ub(2)
Ub(1)
VHL

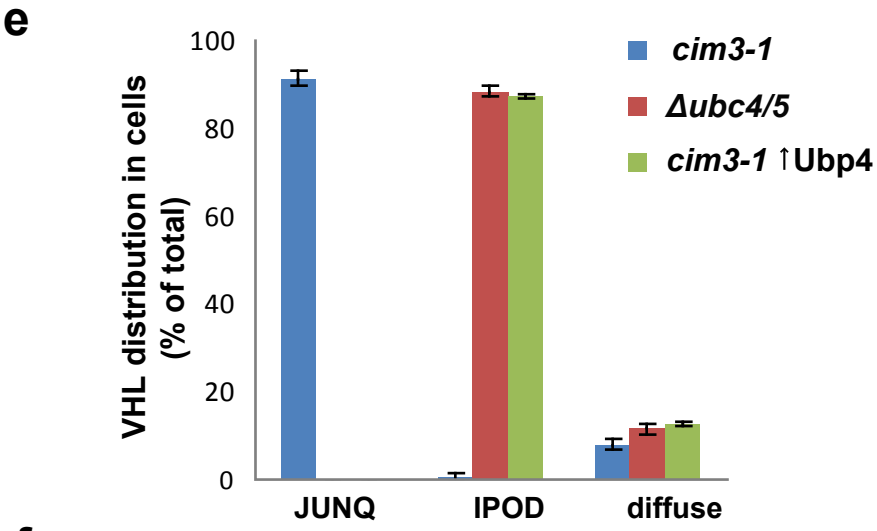
e
VHL distribution in cells (% of total)
100
80
60
40
20
0
JUNQ
IPOD
diffuse
cim3-1
Δubc4/5
cim3-1 ↑Ubp4

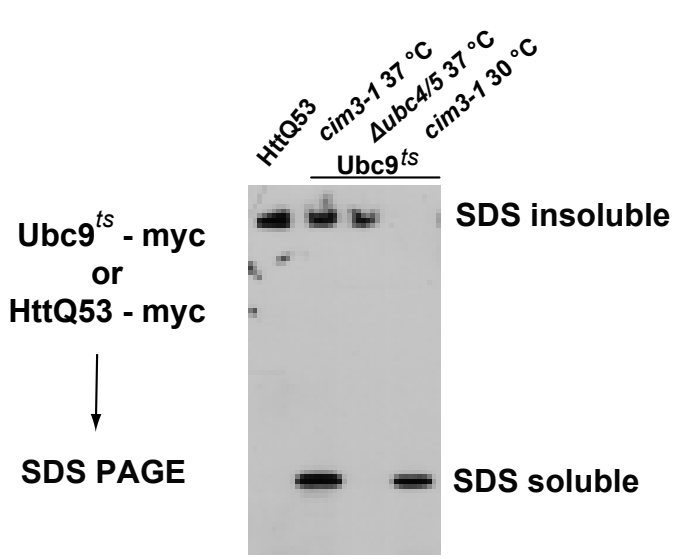
f
HttQ53
cim3-1 37 °C
Δubc4/5 37 °C
cim3-1 30 °C
Ubc9ts
Ubc9ts - myc
or
HttQ53 - myc
SDS PAGE
SDS insoluble
SDS soluble

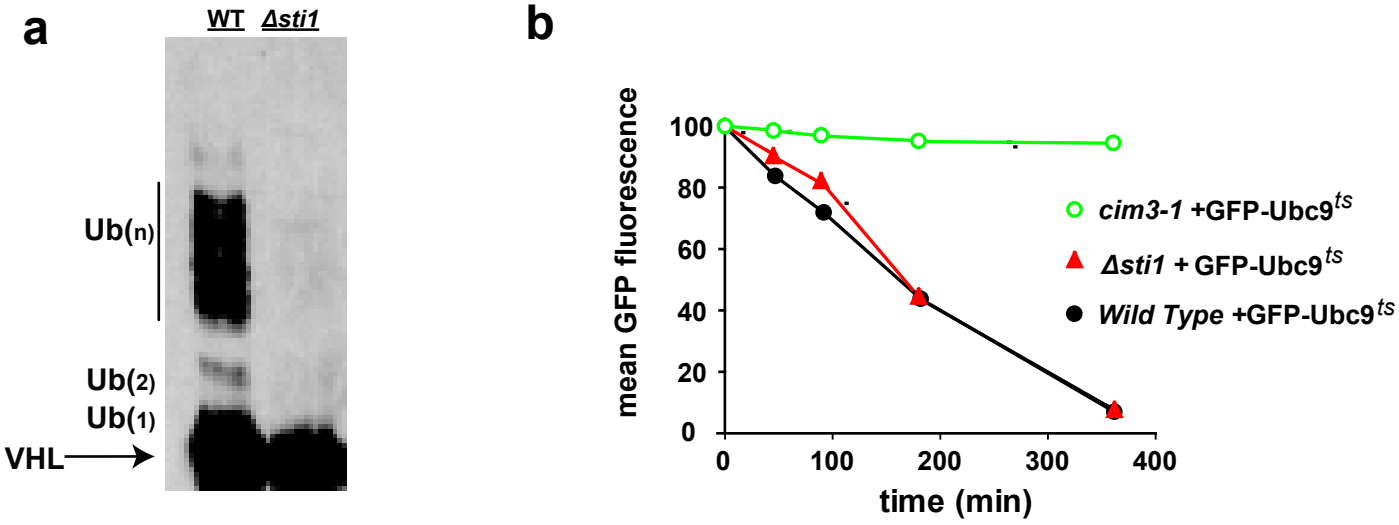
a
WT
Δsti1
Ub(n)
Ub(2)
Ub(1)
VHL
b
mean GFP fluorescence
time (min)
cim3-1 +GFP-Ubc9ts
Δsti1 + GFP-Ubc9ts
Wild Type +GFP-Ubc9ts
c
GFP-VHL
Δsti1
30°C
37°C
IPOD
GFP-Ubc9ts
25°C
37°C 15min
37°C 60min
d
Δsti1 30°C GFP-VHL
IPOD
V
e
VHL
Atg8
merge
IPOD
f
cim3-1
30°C
↑Ubp4
CHFP-VHL
Hsp104-GFP
merge
IPOD

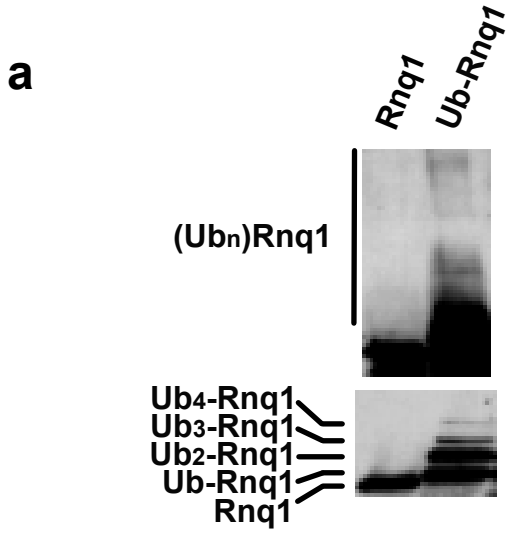
a
Rnq1
Ub-Rnq1
(Ubn)Rnq1
Ub4-Rnq1
Ub3-Rnq1
Ub2-Rnq1
Ub-Rnq1
Rnq1

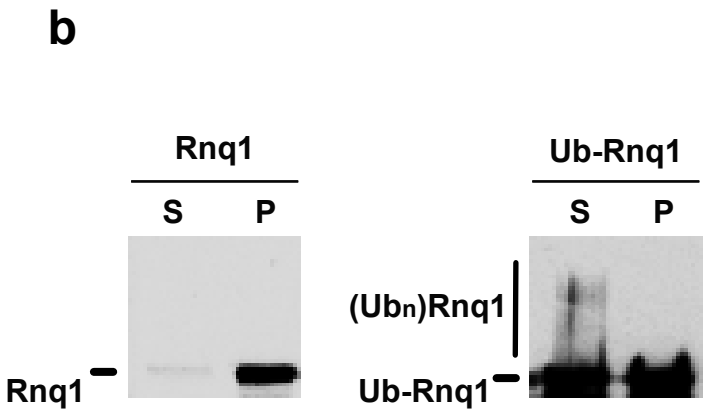
b
Rnq1
S
P
Rnq1
Ub-Rnq1
S
P
(Ubn)Rnq1
Ub-Rnq1

Ubiquitination determines the partitioning of misfolded proteins between two quality control compartments

Daniel Kaganovich, Ron Kopito and Judith Frydman

Supplementary Figure Legends

Figure S1. Proteasome inhibition causes inclusion formation for misfolded proteins, whereas native ubiquitinated proteins remain soluble.

a, Proteasome inhibition causes accumulation of GFP-Ubc9^{ts} in two inclusions. GFP-Ubc9^{ts} expressed in the *cim3-1* proteasome mutant strain and shifted to 37 °C for 1hr or in *Δpdr5* cells, lacking the Pdr5 transporter, and treated with 80μM MG132 for 1hr at 37 °C.

b, Native, correctly folded substrates of the ubiquitination pathway Ub-Arg-GFP and Ub-G76A-GFP exhibit diffuse fluorescence at 37 °C upon proteasome impairment in the *cim3-1* proteasome mutant strain.

c, Upon proteasome inhibition with MG132, the diffuse fluorescence of GFP-VHL is re-distributed to a juxtanuclear inclusion.

d, In mammalian cells, CHFP-VHL and GFP-Ubc9^{ts} form co-localizing peri-nuclear puncta and inclusions next to the ER following 4hr treatment with 10μM MG132 (upper panel). In contrast, GFP-Ubc9^{wt} remains diffuse and does not accumulate in inclusions in similar conditions (lower panel).

e, Deconvolution shows that HttQ103 does not co-aggregate with VHL in mammalian cells.

Figure S2. Benomyl reversibly disrupts ordered inclusion formation.

a, Accumulation of Ubc9^{ts} in two inclusions following misfolding and stress requires microtubule polymerization. *cim3-1* yeast expressing GFP- Ubc9^{ts} were incubated with or without Benomyl for 2hrs at 37 °C. Benomyl causes inclusion formation to arrest at the puncta stage (Top).

b, Puncta formed by misfolded GFP-Ubc9^{ts} in *cim3-1* yeast require microtubule polymerization to coalesce into inclusions. Benomyl addition after puncta had already formed was equally effective in arresting inclusion formation at the puncta stage.

c, Restoring microtubule polymerization after Benomyl arrest by washing out the drug leads to coalescence of puncta into two inclusions.

Figure S3. Biochemical analysis of solubility of native and misfolded proteins upon inhibition of the ubiquitin-proteasome system.

a, Accumulation of VHL in the IPOD corresponds to its accumulation in a Triton-insoluble fraction. Proteasome impaired (*cim3-1*) yeast expressing VHL were incubated at 30 °C (where VHL accumulates only in the JUNQ), or at 37 °C (where VHL also accumulates in the IPOD). Solubility was assessed by a sup/pellet assay as described in Methods.

b, A native proteasome substrate, Ub-GFP, remains soluble at 37 °C in proteasome-mutant (*cim3-1*) yeast.

c, Ub-GFP remains in the soluble fraction in *Δubc4/5* cells, where its ubiquitination is blocked.

Figure S4. Co-localization of QC components with the JUNQ and IPOD compartments.

a, JUNQ and IPOD formed by GFP-Ubc9^{ts} in a dividing *cim3-1* yeast cell, after 2hrs at 37 °C. DNA is stained with DAPI (blue), and the nucleus is stained with NLS-TFP (red). Images were collected as a Z-series and de-convoluted. A 2D projection is shown.

b, JUNQ and IPOD formed by GFP-Ubc9^{ts} in a dividing *cim3-1* yeast cell, after 2hrs at 37 °C, co-expressed with the Sec63-CHFP ER marker. A direct fluorescence image (Top) and a de-convoluted image (Bottom) are shown for **b-g**.

c, The JUNQ compartment (CHFP-VHL, red co-localizes with GFP-labeled proteasomes (Cim5-GFP for regulatory particle, green). VHL accumulation in the JUNQ was induced by proteasome inhibition with MG132.

d, The JUNQ compartment (CHFP-VHL, red), but not the IPOD, co-localizes with GFP-labeled proteasomes (Pre6-GFP for core particle, green). VHL accumulation in the JUNQ was induced by proteasome inhibition with MG132 and IPOD formation was induced by 1hr incubation at 37 °C.

e, The JUNQ compartment, but not the IPOD, co-localizes with GFP-labeled proteasomes (Cim5-GFP for regulatory particle, green). JUNQ and IPOD were formed by Act1-E364K-CHFP over-expression without proteasome inhibition.

f, The JUNQ and the IPOD compartments co-localize with GFP-Hsp104, with the majority of the Hsp104 accumulating around the IPOD. JUNQ and IPOD were formed by expressing CHFP-Ubc9^{ts} in *cim3-1* cells, followed by 1hr incubation at 37 °C.

g, The JUNQ and the IPOD compartments formed by GFP-VHL co-localize with GFP-Hsp104, with the majority of the Hsp104 accumulating around the IPOD.

Figure S5. Characterization of JUNQ and IPOD compartments.

a, EM analysis of JUNQ and IPOD. The JUNQ, shown in the upper panel with GFP-VHL, is formed in a distinct nuclear-membrane associated compartment. Immuno-gold labeled GFP-VHL consistently accumulates in juxta-nuclear protrusions which are adjacent to vacuolar lobes and contain proliferations of the nuclear membrane (white arrows). The IPOD, shown in the lower panels with GFP-Ubc9^{ts}, often is associated with membrane structures (left), and often contains a non-GFP reactive core of densely aggregated proteins (right). A corresponding GFP-fluorescence image is shown in the inset for Ure2.

b, Additional Immuno-EM images of JUNQ (left panels) and IPOD (right panel). The IPOD, shown for Ure2, often is associated with membrane structures, and often localizes next to vacuoles and autophagic vesicles (white arrow).

c, Autophagic components are not required for IPOD formation. Atg7 and Atg8, essential autophagic components, are not required for IPOD formation. GFP-VHL was induced to accumulate in IPODs by Ubp4 over-expression (control in *cim3-1* cells shown in right panels).

Figure S6. Role of ubiquitination in the solubility and partitioning of misfolded proteins to JUNQ and IPOD.

a, Misfolded proteins are ubiquitinated prior to proteasomal degradation. For the QC substrates studied here, ubiquitination can be blocked by over-expression of the Ubp4 ubiquitin hydrolase or by deletion of Ubc4/5.

b, Blocking ubiquitination of misfolded GFP-VHL and GFP-Ubc9^{ts} prevents their localization to JUNQ, and redirects these proteins to the IPOD. The proteasome was blocked by expression in *cim3-1* cells, ubiquitination was blocked by expression in *Δubc4/5* cells or by over-expression of Ubp4, as indicated.

c, Blocking ubiquitination of GFP-Ubc9^{ts} results in its direct targeting to the IPOD. Localization patterns of folded and misfolded GFP-Ubc9 in MHY501 wild-type yeast and *Δubc4/5/6/7* yeast are shown. GFP-Ubc9^{ts} was detected by direct fluorescence for all images as in Figure 1. Nuclei were visualized by co-expressing NLS-TFP from a bi-directional promoter on the same plasmid as GFP-Ubc9^{ts}.

d, Hsp104 localizes around IPODs containing misfolded VHL.

e, Ubiquitinated VHL accumulates upon expression in proteasome-mutant *cim3-1* cells (left panel). Deletion of *Δubc4/5* drastically decreases the amount of VHL-ubiquitin conjugates as compared to wild-type (right panel).

f, Quantification of VHL aggregation phenotypes. The results of microscopy experiments are represented in the graphs shown. Graphs represent three separate experiments in which 100 cells were counted at each time-point. Error bars represent the standard error mean of three experiments.

g, Accumulation of Ubc9^{ts} in the IPOD, after incubation at 37 °C in *cim3-1* cells, or *Δubc4/5* cells corresponds to its accumulation in an SDS-insoluble fraction which fails to fully enter the resolving phase of a 12% SDS gel, similar to HttQ53.

Figure S7. Specific role of the Sti1 chaperone in recruitment of misfolded VHL but not Ubc9^{ts} to the JUNQ.

- **a,** Expression of VHL in a *Δsti1* strain leads to decreased ubiquitination.
- **b,** Sti1 is not required for Ubc9^{ts} degradation (a timecourse of mean GFP fluorescence as analyzed by FACS sorting is shown). Direct fluorescence images of GFP-Ubc9^{ts} in *Δsti1* cells after shift to 37 °C is shown.
- **c,** Deletion of the Sti1 chaperone, required for VHL degradation, results in re-routing of misfolded VHL to the IPOD.
- **d,** EM analysis shows Immuno-gold labeled GFP-VHL consistently localizing to IPOD in *Δsti1* mutant.
- **e,** Co-localization between GFP-VHL and CHFP-Atg8 is shown in the *Δsti1* strain, lacking a chaperone required for misfolded VHL degradation.

Figure S8. A synthetic signal to promote Rnq1 ubiquitination enhances its solubility.

- **a,** Addition of a ubiquitination signal (Ub-G76A) to Rnq1 results in its increased ubiquitination.
- **b,** Enhancing the ubiquitination of Rnq1 leads to the re-distribution of some of the prion protein to a detergent-soluble fraction. Note that the poly-ubiquitinated Ub-Rnq1 is found entirely in the soluble fraction.

Legends to Supplementary Movies

Supplementary Movie 1

Folding incompetent Act1-E364 (green, tagged with GFP) co-localizes with Ubc9^{ts} (red, tagged with CHFP) in *cim3-1* yeast, after 2hrs at 37 °C. Images were collected as a Z-series and de-convoluted. A 3D 180° projection is shown.

Supplementary Movie 2

Co-localization of inclusions of HttQ103 (green, tagged with GFP) with Ubc9^{ts} (red, tagged with CHFP) in *cim3-1* yeast, after 2hrs at 37 °C. Images were collected as a Z-series and de-convoluted. A 3D 180° projection is shown.